

## STRUCTURAL ANOMALIES, OXYGEN ORDERING AND SUPERCONDUCTIVITY IN OXYGEN DEFICIENT $\text{Ba}_2\text{YCu}_3\text{O}_x$

R.J. CAVA<sup>a</sup>, A.W. HEWAT<sup>b</sup>, E.A. HEWAT<sup>c</sup>, B. BATLOGG<sup>a</sup>, M. MAREZIO<sup>d,a</sup>, K.M. RABE<sup>e</sup>,  
J.J. KRAJEWSKI<sup>a</sup>, W.F. PECK Jr.<sup>a</sup> and L.W. RUPP Jr.<sup>a</sup>

<sup>a</sup> *AT&T Bell Laboratories, Murray Hill, New Jersey 07974, USA*

<sup>b</sup> *Institut Laue-Langevin, 156X, 38042 Grenoble Cedex, France*

<sup>c</sup> *Centre d'Etudes Nucleaires de Grenoble, 85X, 38041 Grenoble Cedex, France*

<sup>d</sup> *Laboratoire de Cristallographie, CNRS, 166X, 38042 Grenoble Cedex, France*

<sup>e</sup> *Department of Applied Physics, Yale University, New Haven, Connecticut 06520, USA*

Received 21 November 1989

Revised manuscript received 15 December 1989

We report the characterization of series of oxygen deficient  $\text{Ba}_2\text{YCu}_3\text{O}_x$  samples for  $7 \geq x \geq 6$  prepared by Zr gettered annealing at 440°C. Measurements include complete crystal structure analysis at 5 K by powder neutron diffraction, electron microscopy study of the oxygen ordering, and magnetic measurements of the superconducting transitions, with particular attention to the transition widths. The results show for the first time that the 90 K and 60 K plateaus in  $T_c$  as a function of oxygen stoichiometry are associated with plateaus in the effective valence of the plane coppers. We also correlate the disappearance of superconductivity for  $x < 6.5$  with an abrupt transfer of negative charge into the  $\text{CuO}_2$  planes. We propose that different ordering schemes of oxygen have different characteristic  $T_c$ 's between 90 and 60 K.

### 1. Introduction

The variations of physical properties with oxygen stoichiometry in the  $\text{Ba}_2\text{YCu}_3\text{O}_x$  superconductor has proven to be of considerable interest. As the oxygen content changes from 7 to 6,  $\text{Ba}_2\text{YCu}_3\text{O}_x$  exhibits structural transitions, two plateaus near 90 K and 60 K in the superconducting transition temperatures, the disappearance of superconductivity, and the onset of antiferromagnetism. The variation of oxygen content involves only the population and depopulation of one oxygen site, along the copper-oxygen chains. After many experimental studies, the detailed behaviour of oxygen deficient  $\text{Ba}_2\text{YCu}_3\text{O}_x$  remains controversial (see for instance, refs. [1-9]). In particular, the exact stoichiometries where the changes occur depend sensitively on the technique of material preparation. This is because for intermediate values of  $x$  there are many possible metastable microscopic oxygen arrangements in the region of the chain coppers. Thus, two samples with the same oxygen content can differ substantially in the pres-

ence or nature of the microscopic oxygen ordering, giving rise to differences in observed structural parameters and electronic behaviour. For a given total oxygen content, the oxygen may be long or short range ordered, or disordered. Disordering of the oxygen sublattice involves the movement of some of the oxygen from the chain positions to the nearby vacant oxygen sites.

When  $\text{Ba}_2\text{YCu}_3\text{O}_7$  is heated to temperatures above 500°C it loses oxygen. Heating  $\text{Ba}_2\text{YCu}_3\text{O}_7$  to temperatures between 500°C and 900°C and quenching to ambient temperature is a natural way to prepare oxygen deficient samples, and is, in fact, the manner by which most samples have been made. After a rapid quench, the microscopic state of the oxygen sublattice is therefore the frozen-in high temperature equilibrium state, an equilibrium state which is strongly influenced by the entropy introduced by the elevated temperatures employed. Preparing oxygen deficient samples by quenching them from a wide temperature range produces "equilibrium" oxygen arrays with widely varying entropic contributions. Thus in a se-

ries of samples with varying oxygen content introduced by heating to high temperatures, one has to consider not only the oxygen content, but also the variable entropy term. Such samples show a broad almost featureless variation of  $T_c$  with  $x$ , and a continuous variation in crystallographic cell parameters.

In contrast, the Zr **gettered** annealing technique [ 1 ] allows the synthesis of oxygen deficient  $Ba_2YCu_3O_x$  which has a constant entropic contribution because all stoichiometries can be prepared at the *same* relatively low temperature. Such samples show by far the most distinct 90 K and 60 K plateaus in  $T_c$  and the most abrupt loss of superconductivity near  $x=6.45$ . Because of the long annealing times employed, one would expect to observed tendencies for oxygen ordering, if they exist. By careful analysis of crystallographic cell parameters and superconducting properties for Zr **gettered** samples near  $x=6.5$  it was shown that there is an anomalous increase in the  $c$  lattice parameter at precisely the oxygen stoichiometry where superconductivity disappears [ 6]. Both the change in  $c$  and the disappearance of superconductivity were attributed to an abrupt transfer of charge from the  $CuO$  chains to the  $CuO_2$  planes. Although there were no structural data available for the same Zr **gettered** samples, it was suggested by inspection of other crystallographic data that the internal charge redistribution was sensitively reflected in the plane copper-apical oxygen bondlength, changing both  $c$  and the electrical properties.

Due to the importance of the microscopic oxygen arrangement in determining the physical properties of  $Ba_2YCu_3O_x$ , it is crucial to characterize one particular series of samples as completely as possible in order to make correlations between observed physical properties and microscopic causes. This should include measurements of unit cell parameters, internal atomic position coordinates and superconducting properties. In this paper we describe the results of such a study of a series of Zr **gettered** oxygen deficient  $Ba_2YCu_3O_x$  samples. We measured the diamagnetism due to superconductivity, with particular attention to transition width, performed electron diffraction studies of short range oxygen ordering, and made detailed measurements of bondlengths by powder neutron diffraction. The neutron diffraction results are most important, as they enable us to extend the earlier analysis of correlations between

structural and electronic (superconducting) properties. We have characterized in detail the significant structural anomaly that occurs at the disappearance of superconductivity, and a very subtle structural change at the transition from the 90 K to the 60 IS superconductor. We propose that different vacancy ordering schemes have their own characteristic  $T_c$  between 90 K and 60 K. We also believe that the 60 K plateau reflects the relatively high stability of the "full-empty" chain configuration associated with 6.5 oxygens per formula unit, in agreement with conclusions from a recent electron microscopy study [ 14 ].

## 2. Sample preparation

Single phase polycrystalline  $Ba_2YCu_3O_7$  pellets were prepared as described elsewhere [ 1 ]. Oxygen was then removed from the samples by heating 1.0 g pellets in sealed evacuated quartz tubes of 20  $cm^3$  volume for four days at 440°C with O-14 pieces of 0.5 x 1.0 inch area bright Zr foil. For the largest oxygen deficiencies,  $x=6.35$  and 6.0, the desired oxygen content was not reached after a single annealing step, and so selected samples were re-annealed with new Zr under the same conditions to remove more oxygen. The oxygen content of the samples was derived from the weight change of part of the sample on reduction in  $N_2-15\% H_2$ , according to the chemical formula  $Ba_2YCu_3O_{7-x} + (3.5-x)H_2 \rightarrow 2BaO + 0.5Y_2O_3 + 3Cu + (3.5-x)H_2O_2$ , allowing the determination of oxygen content to an accuracy of 0.02 oxygens per formula unit. Ten samples with oxygen contents spanning the full stoichiometry range were chosen for this study.

## 3. Superconducting properties

The superconducting transition temperatures were measured by DC magnetization (SHE SQUID magnetometer) on small pieces of the polycrystalline pellets on cooling in a field of 5 Oe. The results are shown in fig. 1 and table I, and are in agreement with those obtained on other samples prepared by the same techniques, showing two plateaus, at approximately 90 K and 55 K, and a broad intermediate  $T_c$  region. For this plot,  $T_c$  has been determined in the

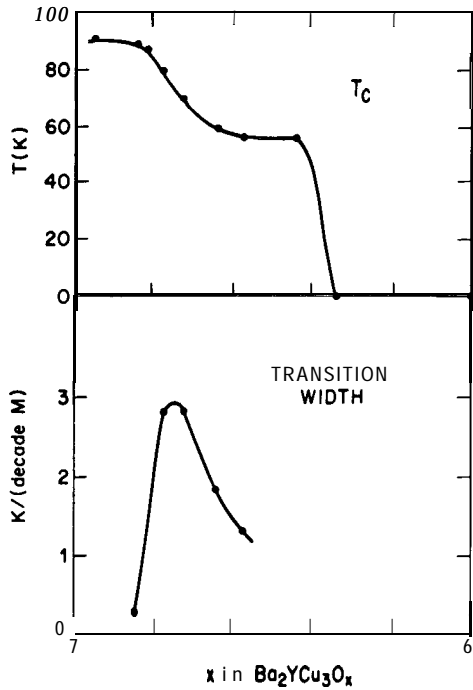


Fig. 1. Superconductive transition temperature  $T_c$  for the ten samples of  $Ba_2YCu_3O_x$  employed in this study. The width of the superconducting transitions in kelvins per decade of magnetization is also shown.

Table I  
Superconducting transition temperatures ( $T_c$ ) and superstructures observed by electron diffraction for  $Ba_2YCu_3O_x$  prepared at 440°C.

| $x$  | $T_c$ (K) | Superstructure  |
|------|-----------|---|
| 6.95 | 90        | none  |
| 6.84 | 88        | none  |
| 6.81 | 86        | diffuse lines   |
| 6.73 | 69        | diffuse lines + diffuse $3a$ spots                            |
| 6.64 | 59        | elongated $2a$ spots; some diffuse $3a$ , some $\frac{1}{4}0$ |
| 6.58 | 56        | sharp $2a$ spots  |
| 6.45 | 56        | sharp $2a$ spots  |

usual way by the onset of diamagnetism on a linear scale. More insight, however, can be gained in more sensitive measurements, described in a later section. The superconducting transitions are sharpest in the composition regions of the plateau (fig. 1). Superconductivity abruptly disappears for  $x < 6.45$ , with good bulk Meissner signals (greater than 50% of the theoretical values) for all samples  $x \geq 6.45$ .

#### 4. Oxygen ordering

Electron microscopy investigations of these samples were carried out on a JEOL 400CX EM. All samples were very finely ground, so that even the larger crystallites had nicked edges, with smaller crystallites ( $\approx 10$  nm) adhering to their surfaces. Results are summarized in table I. The edges of samples with  $x=6.58$  and  $x=6.45$  had some damaged regions with stacking faults showing double CuO chains as in  $YBa_2Cu_4O_8$ . For  $7 > x > 6.84$ , no superstructure or diffuse scattering was observed (fig. 2a). For  $x=6.81$  and 6.73, diffuse lines along  $[100]$  through the  $h0l$  spots were observed in some grains, showing highly uncorrelated full-empty chain ordering. For  $x=6.73$  and 6.64, diffuse  $3a$  spots were observed in a few grains. Very elongated  $2a$  spots were also present in nearly all grains (fig. 2b) for  $x=6.64$ , a few grains also showed well defined  $\frac{1}{4}0$  spots. The  $2a$  spots became sharp in  $x=6.58$  and  $x=6.45$  samples (fig. 2c), and the  $[010]$  diffraction patterns (fig. 2d) showed that these superlattice spots were also sharp along the  $c$ -axis. Therefore the superstructure in these samples near  $Ba_2YCu_3O_{6.5}$  is well ordered in all three directions. In samples prepared by the standard technique of quenching from higher temperatures, the superstructure order is absent along the  $c$ -axis, and diffuse  $[001]$  streaks through  $h+\frac{1}{2}, 0, l$  are observed (see for instance, refs. [1, 10–16]), sometimes showing intensity modulation with maxima at integer values of  $l$ .

The  $2a$  superstructure is believed to be caused by complete absence of oxygen from every second CuO chain. The neutron diffraction on these samples did not detect the expected superlattice reflections even though the electron microscopy results indicate that this superstructure is well ordered in three directions in the range  $6.6 < x < 6.4$ , corresponding to the plateau in the  $T_c$  curve (fig. 1). Outside this composition range, ordering of oxygen vacancies is very short range. The  $T_c=60$  K plateau can then be associated with a well defined intermediate structure corresponding to the phase  $Ba_2YCu_3O_{6.5}$ . We note that both superconductivity and electron diffraction require a relatively small coherence volume for the observation of a distinct "phase". The coherence volume for the well ordered  $Ba_2YCu_3O_{6.5}$  phase commonly produced is apparently smaller than is required for its observation by neutron diffraction.

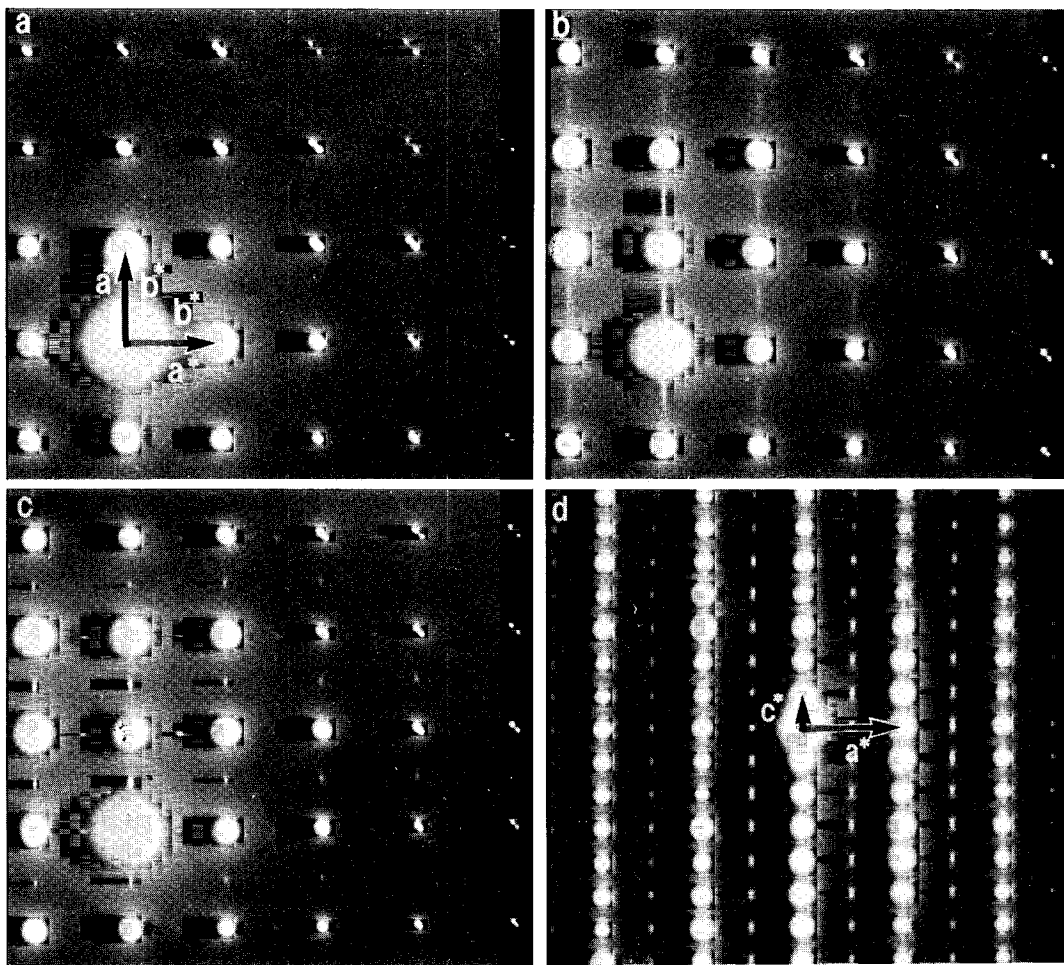


Fig. 2. Electron diffraction patterns from orthorhombic  $Ba_2YCu_3O_x$  showing: (a) typical twinning with no diffuse scattering for  $x > 6.8$ , (b) short range superstructure for  $x = 6.64$ , (c) long range superstructure in the x-y plane for  $6.58 \geq x \geq 6.45$ , (d) long range order also along the c-axis for  $6.582 < x < 6.45$ .

## 5. Neutron diffraction

The samples, sintered disks approximately 10 mm in diameter and 1 mm thick, were sealed in a vanadium can with the disk normal to the incident neutron beam. All measurements were made on D2B [17] at ILL in a helium flow cryostat at 5 K, with eight one-hour scans averaged over different detectors for each sample. The wavelength of 1.5946(3) Å was chosen to maximize the count rate, at the expense of fewer reflections than were obtained for example by Francois et al. [18]. The statistics for the  $x = 6.45$  sample are a little poorer because the sample was broken, and the piece used was only about half

the size of the other samples: this had little effect on the precision of the structural parameters. All samples were positioned at approximately the same point in the neutron beam, since this determines the effective wavelength. Possible positioning errors are responsible for the estimated error limits of  $\pm 0.0003$  Å in the neutron wavelength, which is the largest source of the absolute error in the determination of the lattice dimensions.

The data were analyzed using an early version of the Rietveld profile refinement program [19], with the labeling of atoms followed that of Capponi et al. [20] (fig. 3). Since all measurements were at low temperature, isotropic temperature factors  $B$  were

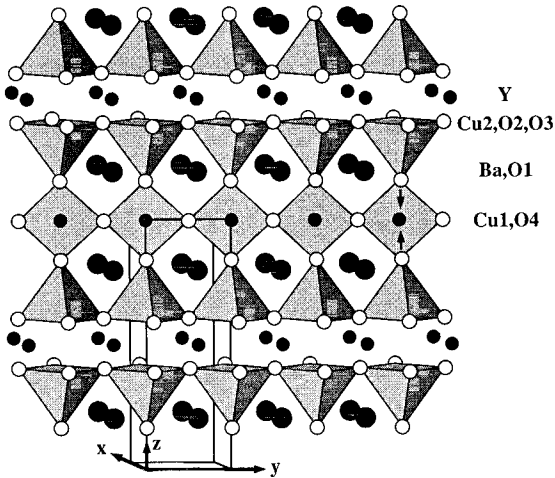


Fig. 3. The structure of  $Ba_2YCu_3O_7$ , showing the atom labels used in the present paper.

used for all atoms. No attempt was made to refine a double minimum site for the chain oxygen O(4), as done by Francois et al. [ 18 ], because the longer

wavelength employed meant that such details could not be resolved. The oxygen occupancies were refined for all sites and all samples, all sites except O4 appeared fully occupied to within the calculated standard errors – about 3% for oxygen occupancy. The standard error was larger for O( 4 ), because of the smaller scattering power of the partially occupied site, and because of the usual correlation with its temperature factor. The occupancy of the site O( 4 ) increased above its nominal value slightly when refined, compensated by an increase in the B-factor. However, it was finally concluded that there was no evidence that the occupancies of the oxygen sites were other than their nominal values (i.e. fully occupied for all sites except O( 4 ), and O( 4 ) occupancy as determined from the measured stoichiometry ). Occupancies were therefore kept fixed for the final refinements. There was no evidence for significant oxygen occupancy of the oxygen (  $\frac{1}{2}$ 00 ) sites along the u-axis. Fig. 4 demonstrates the generally good agreement obtained between the observed and cal-

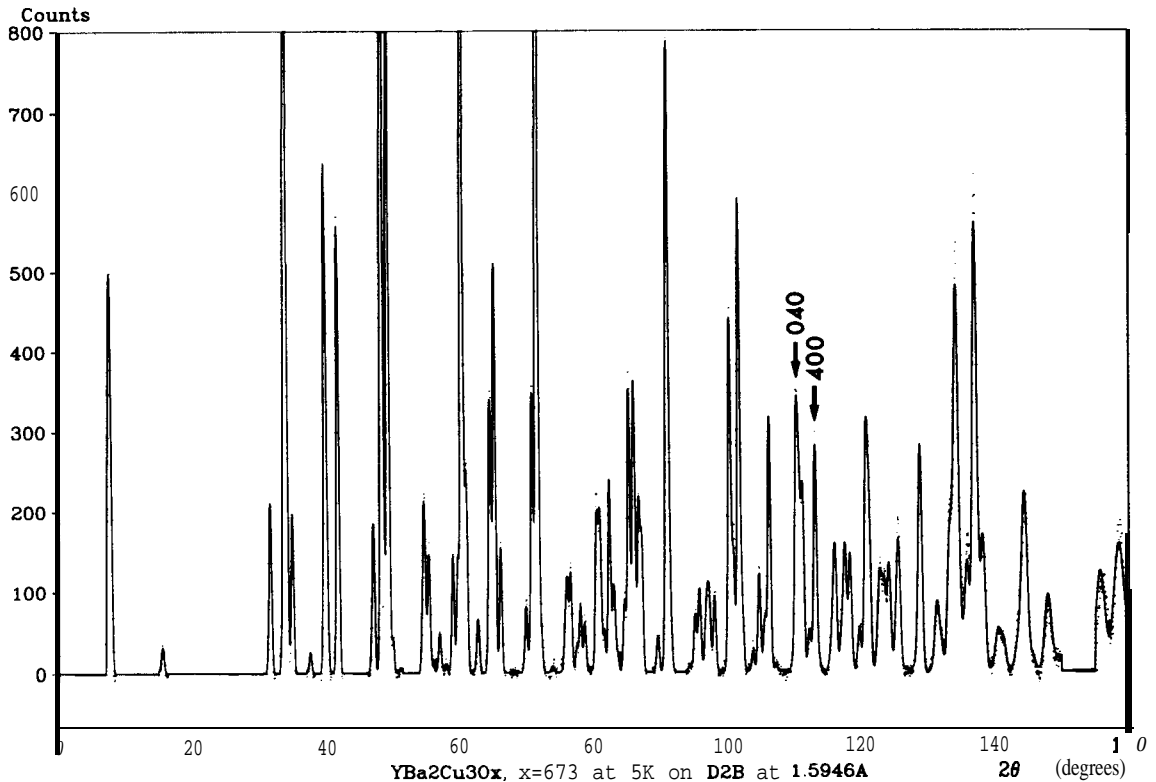


Fig. 4. Observed (points) and calculated neutron diffraction patterns for  $Ba_2YCu_3O_{6.73}$  at 5 K. The arrows show the clear separation of the 040 and 400 reflections due to the orthorhombicity of the structure.

Table II  
Structural parameters at 5 K for  $YBa_2Cu_3O_x$  with various oxygen stoichiometries. The relative cell dimensions  $a$ ,  $b$ ,  $c$  are reliable within the quoted standard deviations, but these do not include the uncertainty in the effective neutron wavelength  $\lambda = 1.5946(3) \text{ \AA}$ .

| $x =$ | 6.95       | 6.84       | 6.81       | 6.78       | 6.73       | 6.64       | 6.58       | 6.45       | 6.35       | 6.00       |
|-------|------------|------------|------------|------------|------------|------------|------------|------------|------------|------------|
| $a$   | 3.8136(1)  | 3.8153(1)  | 3.8163(1)  | 3.8170(1)  | 3.8193(1)  | 3.8224(1)  | 3.8252(1)  | 3.8293(1)  | 3.8580(1)  | 3.8544(1)  |
| $b$   | 3.8845(1)  | 3.8848(1)  | 3.8845(1)  | 3.8836(1)  | 3.8835(1)  | 3.8811(1)  | 3.8786(1)  | 3.8750(1)  | 3.8580(1)  | 3.8544(1)  |
| $c$   | 11.6603(3) | 11.6692(3) | 11.6739(3) | 11.6768(3) | 11.6832(2) | 11.6912(3) | 11.6987(3) | 11.7101(4) | 11.7913(3) | 11.8175(4) |
| Ba    | 0.1843(2)  | 0.1856(2)  | 0.1859(2)  | 0.1862(2)  | 0.1867(2)  | 0.1873(3)  | 0.1877(2)  | 0.1878(3)  | 0.1931(2)  | 0.1944(3)  |
| Y     | 0.34(4)    | 0.41(4)    | 0.25(4)    | 0.27(40)   | 0.32(3)    | 0.16(5)    | 0.43(4)    | 0.05(6)    | 0.68(6)    | 0.37(6)    |
| Cu(1) | 0.44(4)    | 0.43(4)    | 0.44(4)    | 0.18(4)    | 0.37(3)    | 0.18(5)    | 0.63(4)    | 0.14(6)    | 0.48(5)    | 0.15(5)    |
| Cu(2) | 0.3546(2)  | 0.3552(1)  | 0.3561(1)  | 0.26(4)    | 0.29(3)    | 0.11(4)    | 0.46(4)    | 0.06(6)    | 0.76(5)    | 0.44(5)    |
| O(1)  | 0.22(3)    | 0.28(3)    | 0.17(3)    | 0.14(3)    | 0.23(2)    | 0.01(3)    | 0.47(3)    | 0.09(4)    | 0.59(3)    | 0.23(3)    |
| O(2)  | 0.65(4)    | 0.71(4)    | 0.65(4)    | 0.55(4)    | 0.68(3)    | 0.51(4)    | 0.86(4)    | 0.54(6)    | 1.06(5)    | 0.61(5)    |
| O(3)  | 0.3777(2)  | 0.3777(2)  | 0.3785(2)  | 0.3787(2)  | 0.3786(2)  | 0.3786(2)  | 0.3792(2)  | 0.3781(3)  | 0.3788(2)  | 0.3791(2)  |
| O(4)  | 0.97(8)    | 0.72(8)    | 0.56(8)    | 0.49(8)    | 0.31(3)    | 0.38(4)    | 0.74(4)    | 0.30(6)    | 0.59(3)    | 0.27(3)    |
| $R_r$ | 0.475      | 0.420      | 0.405      | 0.390      | 0.375      | 0.65(11)   | 0.86(10)   | 0.10(6)    | 0.59       | 0.27       |
| $R_p$ | 6.57       | 8.14       | 7.32       | 5.61       | 4.46       | 0.320      | 0.290      | 0.225      | 0.175      | 0.000      |
|       | 10.42      | 9.32       | 10.61      | 9.85       | 8.03       | 10.92      | 9.50       | 15.51      | 12.63      | 12.93      |

culated diffraction patterns, showing that the statistics are adequate, and that peaks are well resolved for the whole of the diffraction pattern. Fig. 4 also shows that the splitting between the 040 and 400 peaks is clearly resolved. The orthorhombicity of the samples is therefore well determined.

The refined structure parameters are given in table II, where the quoted errors for the lattice constants do not include the overall error in the wavelength. The atomic coordinates are very precise, but the atomic temperature factors  $B$  are less so. The  $R_I$ -factor is for integrated peak intensities, and is given for comparison with the conventional crystallographic  $R_F = 0.5 R_I$ . The profile  $R_p$ -factor was minimized in the refinement. The R-factors are somewhat larger for the  $x < 6.4$  samples, which showed some weak impurity lines.

## 6. Crystal structure

In fig. 5, the crystallographic cell parameters are shown as a function of stoichiometry. As for other samples prepared by Zr gettering, there is a distinct

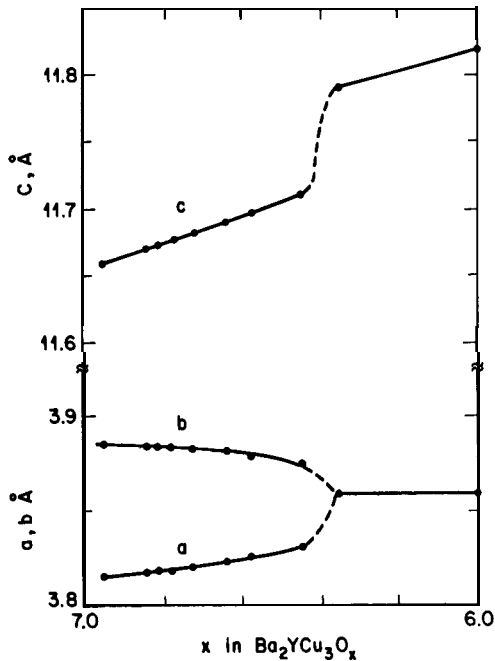


Fig. 5. Refined crystallographic cell parameters for  $Ba_2YCu_3O_x$  prepared by Zr gettering at 440°C.

step-like increase in the c-axis length near a stoichiometry of 6.4 oxygens per formula unit. Earlier work [6] showed that the exact stoichiometry where this step occurs depends on the annealing temperature. In this series we do not have samples in which the c anomaly has occurred within the orthorhombic symmetry phase, although in the earlier study it was shown that the c-axis step and the orthorhombic to tetragonal transition do not necessarily occur at the same composition. Fig. 6 shows, as a function of oxygen content, the step-like increase in cell volume, and the change in orthorhombicity, a measure of the difference in lengths between the a- and b-axes. Note that the orthorhombicity is not a linear function of stoichiometry that would extrapolate to zero at  $x=6.0$  if there were no orthorhombic-tetragonal phase transition. This is due to the cooperative phenomena which tend to maintain the integrity of the chains as oxygen is removed. It has been shown earlier that the variation of orthorhombicity with oxygen content depends on the annealing temperature [6].

With the structural refinements from the neutron

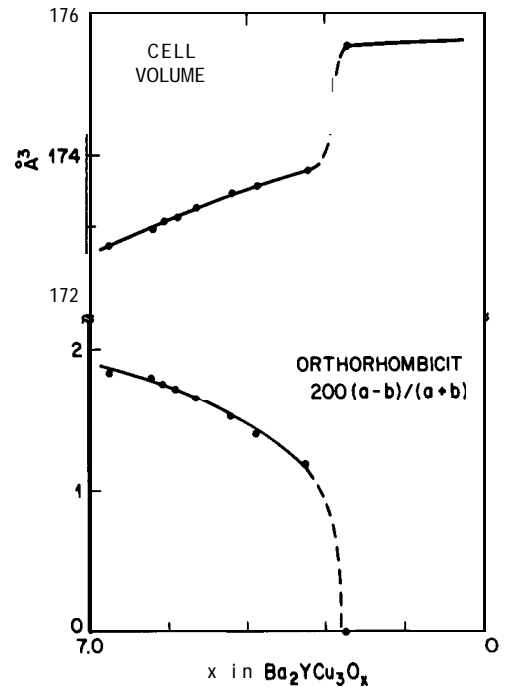


Fig. 6. Crystallographic cell volume and orthorhombicity for  $Ba_2YCu_3O_x$  prepared by Zr gettering at 440°C.

diffraction data, we can for the first time obtain a detailed picture of the oxygen stoichiometry dependence of the relative positions of the atoms in the unit cell for the low temperature annealed samples. The structures obtained are positional averages over all the microscopic configurations present at a particular composition. For example, with the exception of the end members  $x=6$  and  $x=7$ , the atomic positions for Ba and the chain coppers Cu (1) are averaged over several different oxygen coordination numbers. The observed coordination polyhedron around the plane copper Cu (2) is also an average over microscopic configurations depending on whether the Cu (1) neighbour sharing the apical oxygen has four oxygen neighbours, or is in an "empty" chain and therefore two-coordinated. The electron diffraction study shows that for low oxygen deficiencies the averages in position are over small numbers of randomly distributed vacant oxygen sites. For intermediate oxygen deficiencies, until the orthorhombic to tetragonal transition, the positional averages are over short range ordered arrangements of fully occupied copper chains and empty copper chains in different ratios. In the tetragonal phase, the distribution of oxygens in the Cu(1) chain layers is in short orientationally disordered full chain fragments. The relatively well ordered nature of the low temperature annealed samples allows us to observe significant and relatively abrupt changes in average positions and physical properties as a function of oxygen stoichiometry.

The next set of figures presents in graphic form the variation of the important cation-oxygen bondlengths as a function of oxygen stoichiometry. Fig. 7 shows that for the chain coppers (Cu(1)) there is relatively little change in bondlength over the whole stoichiometry range. The bondlength to the oxygen in the same plane (O(4)), is virtually unchanged, while the bondlength along *c* shows some variation in the orthorhombic phase. These results are completely consistent with a model in which the "chain" copper site primarily consists of a mixture of twofold (O(1)-Cu(1)-O(1) dumbbells) and fourfold (Cu(1)-O(1)-O(4) squares) coordinations as a function of stoichiometry, with the sticks having shorter Cu(1)-O(1) bondlengths than the diamonds.

The plane coppers (Cu(2)) are coordinated to four

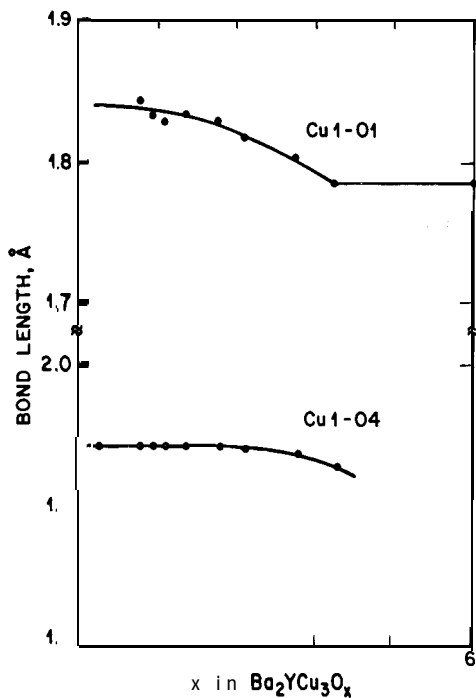


Fig. 7. Chain copper (Cu(1))-oxygen bondlengths, for oxygens in the same plane (O(4)) and the oxygens bridging (O(1)) to the planar copper, as a function of oxygen stoichiometry.

oxygen atoms in the plane (two O(2)'s and two O(3)'s) and one oxygen at the apex of a pyramid (O(1)) which it shares with the chain copper Cu(1). The variation in these bondlengths with stoichiometry is shown in fig. 8. The bondlengths to the plane oxygens are slightly different due to the orthorhombicity for  $x > 6.4$ , and become equal at the orthorhombic to tetragonal transition. The mean bondlength to these plane oxygens shrinks very slightly ( $\approx 0.008$  Å), and insignificantly from an electronic standpoint, as  $x$  decreases from 7 to 6. The bottom of fig. 9 shows that there is a small but significant change in the puckering of the Cu(2)-O(2,3) plane as oxygen is removed from the orthorhombic phase. Fig. 8 shows that there is a very large change in the bondlength to the apical oxygen atom, with a total increase of approximately 0.17 Å, over the stoichiometry range of the compound. As inferred earlier from the step-like increase in the *c*-axis length, the structural data show that the underlying microscopic cause is the step-like increase in the plane copper-apical oxygen bondlength near  $x=6.4$ . This is the com-

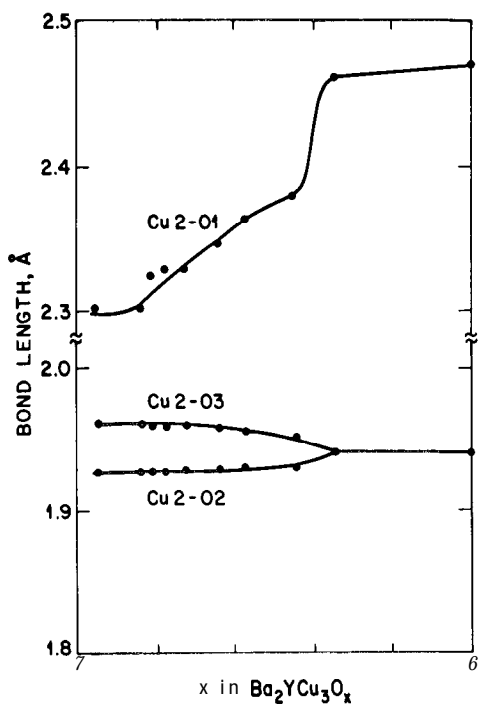


Fig. 8. Plane copper (Cu(2))-oxygen bondlengths for oxygens in the same plane (O(2,3)) and the apical oxygen(O(1)), as a function of oxygen stoichiometry.

position where superconductivity disappears. In addition to the dramatic step near  $x=6.4$ , there is an intermediate step-like behaviour, but broadened, within the orthorhombic phase for  $x > 6.4$ . This variation in bondlength in fact mimics very closely the variation in  $T_c$  versus  $x$  and will be discussed in more detail in what follows.

The barium-oxygen coordination also changes in a step-like manner near the  $x=6.4$  stoichiometry, as shown in figs. 9 and 10. It was proposed earlier that this is best viewed as a polarization of the Ba-0(1) layer in response to the transfer of charge from the chains to the planes at the same composition [6]. The top of fig. 9 shows that it is the puckering, or polarization, of the Ba-0(1) layer that is most strongly affected, even though the actual change in bondlength (fig. 10) is relatively small. Fig. 11 shows that the coordinations of Ba and Y to the plane  $0x-$

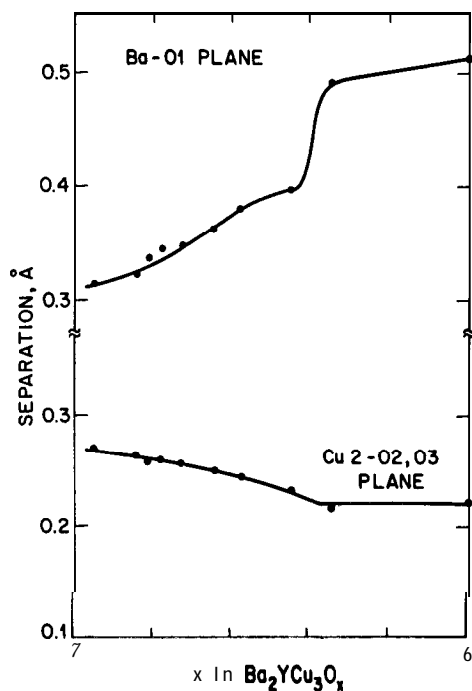


Fig. 9. Puckering of the Ba-0(1) plane and the plane copper-oxygen plane (Cu(2)-O(2,3)) as a function of oxygen stoichiometry.

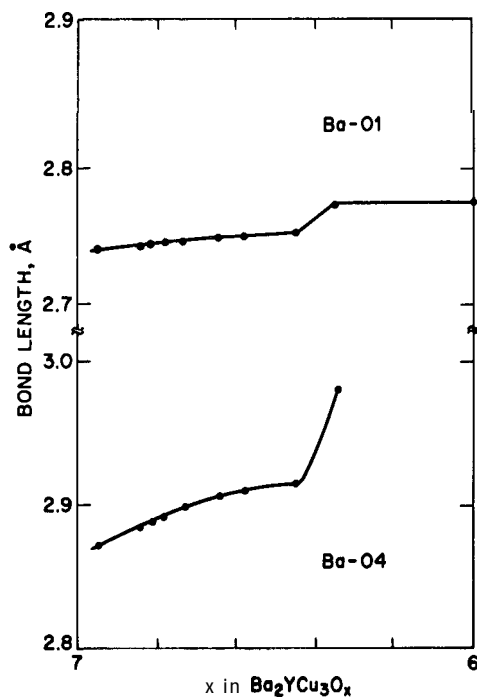


Fig. 10. Barium-oxygen bondlengths as a function of oxygen stoichiometry. ▶

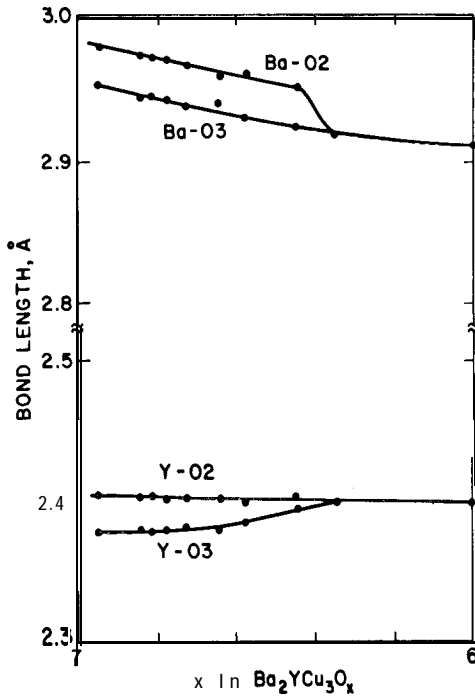


Fig. 11. Bondlengths of Ba and Y to the plane oxygens O (2) and O (3) as a function of oxygen stoichiometry.

ygens O (2) and O (3) merely reflect the change from orthorhombic to tetragonal symmetry, and in the case of Ba a small decrease of the mean bondlength.

## 7. Short range order and superconductivity

The earliest ideas about the manner in which  $T_c$  would depend on oxygen content in  $YBa_2Cu_3O_x$  are now well known to be too simple, as almost all types of sample preparation show the presence of various degrees of plateau structure in plots of  $T_c$  versus  $x$ . As oxygen is removed from the chain sites, it is well established that a series of two or three dimensionally, shorter or longer range ordered superlattices are observed by electron microscopy. These superlattices are assumed to be due to ordering of various numbers "full" and "empty" chains running parallel to  $b$ . Many different ordering schemes with slightly different ratios of full and empty sites are expected to be thermodynamically stable [ 2 1-23 ], and in fact a great variety of superlattices have been ob-

served. The electron microscopy results of this study, as well as many others (especially refs. [ 10 ] and [ 14 ]), point to the following sequence of oxygen ordering microstructures: in the 90 K plateau region, oxygen is generally randomly removed from the chain sites ( $7 \text{ Ix} \leq 6.8$ ). In the region where  $T_c$  is changing from 90 K to 60 K, many kinds of short range ordered full-empty chain arrays are observed, with periodicities near  $3xa$ . Finally at the 60 K plateau, the  $2xa$  long range ordered superlattice dominates. This presumably corresponds to a "full-empty-full-empty..." configuration, which can, under some synthetic conditions be ordered in all three crystallographic directions, as it is for our samples. For some solid solution systems one would expect to see two-phase regions separating the distinct compositions where favourable ordering occurs. For others, a continuous evolution from one ordering periodicity to another can occur through incommensurate periodicities with no composition regions where two distinct phases coexist. For the case of  $YBa_2Cu_3O_x$  in particular there exists no experimental evidence at the present time as to what kind of solid solution is formed. Whatever the case, the fact that the oxygen ordering is only short range over much of the composition range for most synthetic conditions makes the system behave as if it were changing in a continuous manner, with distinctions between the two kinds of solid solution difficult to resolve.

In the composition region between  $x=6.8$  and  $x=6.6$ , two properties of the system are changing quickly, the superconducting transition temperature and the periodicities of the short range ordering of the chain-vacant chain subsystem. It is possible that the rapid change in  $T_c$  is really a short range order broadened progression of distinct  $T_c$ 's, each associated with particular compositions which are very similar. We believe that this is the cause of the dramatic increase in the widths of the superconducting transitions, shown on the bottom of fig. 1. To look at this hypothesis more carefully, we have measured the magnetization over many orders of magnitude in the vicinity of  $T_c$  for the samples in the transition region, from which the data of fig. 1 have been derived. A comparison of the behaviour for several of the samples is presented in figs. 12 and 13. For the  $x=6.84$  sample, on the 90 K plateau, the transition is very sharp. For samples in the intermediate re-

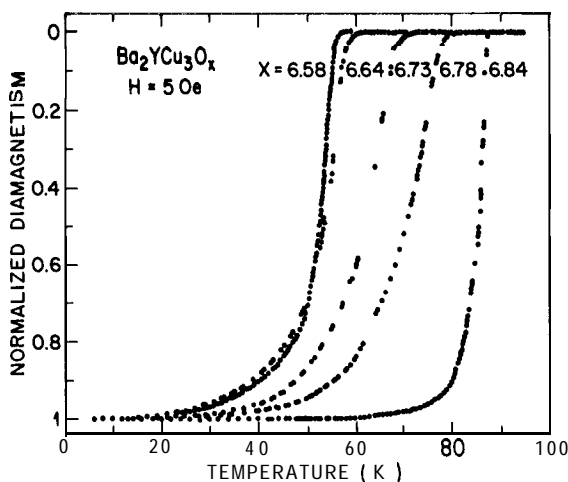


Fig. 12. Superconducting transitions for samples between the 90 K and 60 K plateaus.

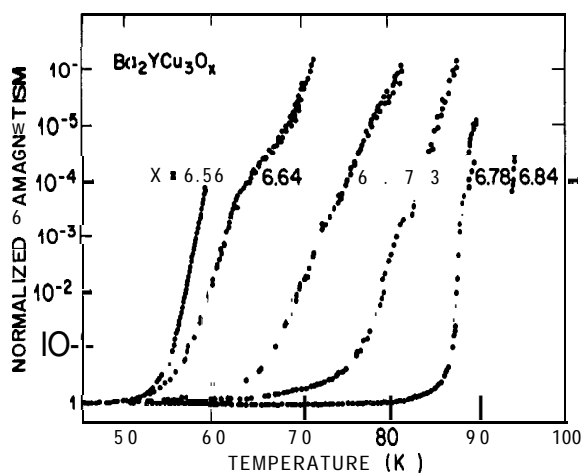


Fig. 13. Superconducting diamagnetism measured over many decades of  $-M$  for samples between the 90 K and 60 K plateaus.

gion,  $6.8 > x > 6.6$ , the transitions are broadened. For one of the samples ( $x=6.4$ ) a multiple transition is observed indicating the coexistence of two phases in this sample with distinct  $T_c$ 's of approximately 71 K and 63 K. This is not the result of inhomogeneity due to poor sample preparation as this sample has been prepared in exactly the same manner as have the samples with very sharp transitions at higher and lower oxygen contents. We therefore interpret the results as being the first observation of distinct  $T_c$ 's in

the composition region of  $6.8 > x > 6.6$ , in support of ideas in which this region of composition could consist of a progression of short range ordered compositions with  $T_c$ 's between 90 K and 60 K. Further careful synthetic work to prepare these compositions with long range ordering would be of considerable interest.

## 8. Bond valence sums

The interatomic distances in crystals are sensitive measures of the amount of charge in the chemical bond between the atoms. There are several effective formulations from which the actual charge in a bond, the "bond strength", can be derived from its bond-length, based on the ideas of Pauling, Zachariasen, and Brown. The relationship between bondlength and bond strength for a particular cation-anion pair is derived empirically from structural information from a large data base of well characterized compounds. The sum of bond strengths around a particular atom is its effective valence. Deviation of the bond strength sum (here called bond valence sum) from the normal valence of a cation not expected to display variable valence such as alkaline earths, is usually considered to reflect an internal stress on the coordination polyhedron of the cation due to geometrical structural constraints imposed by the remainder of the atoms in the structure [25]. Of course, for strongly hybridized systems such as superconducting copper oxides, the bond valence sums for the copper atoms do not represent an ionic but rather covalent bond. The total charge in the bond, however, is a meaningful quantity. For convenience one can calculate the bond valence sums around the cations and talk about the variations in bond charges in terms of the metal "valences" or "bond valence sums".

We have calculated the bond valence sums for the atoms in our  $Ba_2YCu_3O_x$  series from  $V = \sum \exp(R_0 - R_i)/B_i$  where  $R_i$  and  $B_i$  are constants which depend on the atoms, employing the values derived by Brown and Altermatt [24]. Brown has described the application to this particular system in considerable detail [25]. The results are included with the bondlengths in table III, and are illustrated in figs. 14 and 15.

Table III  
Bondlengths in  $YBa_2Cu_3O_x$  at 5 K together with the bond valence sums  $V$  defined by Brown and Altermatt [ 24].

| $x=$  |         | 6.95      | 6.84      | 6.81      | 6.78      | 6.73      | 6.64       | 6.58      | 6.45       | 6.35       | 6.00       |
|-------|---------|-----------|-----------|-----------|-----------|-----------|------------|-----------|------------|------------|------------|
| Ba    | -O(1)×4 | 2.740(0)  | 2.742(0)  | 2.744(0)  | 2.745(0)  | 2.746(0)  | 2.748( 1)  | 2.750(0)  | 2.752( 1)  | 2.772( 1)  | 2.773( 1)  |
|       | -O(2)×2 | 2.980(3)  | 2.973(2)  | 2.972(2)  | 2.971(2)  | 2.966(2)  | 2.960(3)   | 2.963(3)  | 2.952(4)   | 2.918(3)   | 2.911(3)   |
|       | -0(3)×2 | 2.953(3)  | 2.944(3)  | 2.945(3)  | 2.942(3)  | 2.937(3)  | 2.942(4)   | 2.931(3)  | 2.926(4)   | 2.918      | 2.911      |
|       | -0(4)×2 | 2.873(2)  | 2.886(2)  | 2.890(2)  | 2.893(2)  | 2.900(2)  | 2.907(3)   | 2.912(2)  | 2.916(3)   | 2.985(2)   | 2.999(3)   |
|       | - V     | 2.192(7)  | 2.143(6)  | 2.121(6)  | 2.108(6)  | 2.088(5)  | 2.044( 11) | 2.020(6)  | 1.979(11)  | 1.901(8)   | 1.809(8)   |
| Y     | -0(2)×4 | 2.407( 1) | 2.405( 1) | 2.405( 1) | 2.403(1)  | 2.404( 1) | 2.404( 1)  | 2.400( 1) | 2.407(2)   | 2.401( 1)  | 2.399( 1)  |
|       | -0(3)×4 | 2.381(1)  | 2.382( 1) | 2.381(1)  | 2.382(1)  | 2.384( 1) | 2.380(2)   | 2.389( 1) | 2.397(3)   | 2.401      | 2.399      |
|       | - V     | 2.905(7)  | 2.909(7)  | 2.913(7)  | 2.917(7)  | 2.905(7)  | 2.921(11)  | 2.900(7)  | 2.842( 19) | 2.849(7)   | 2.865(7)   |
| Cu(1) | -O(1)×2 | 1.833(2)  | 1.843(2)  | 1.833(2)  | 1.828(2)  | 1.832(2)  | 1.829(2)   | 1.817(2)  | 1.805(4)   | 1.786(4)   | 1.786(4)   |
|       | -0(4)×2 | 1.942(0)  | 1.942(0)  | 1.942(0)  | 1.942(0)  | 1.942(0)  | 1.941(0)   | 1.939(0)  | 1.937(0)   | 1.929(0)   | 1.927(0)   |
|       | - V     | 2.378(7)  | 2.158(6)  | 2.166(7)  | 2.149(7)  | 2.057(7)  | 1.942(7)   | 1.923(7)  | 1.799( 15) | 1.774( 16) | 1.308( 16) |
| Cu(2) | -O(1)×1 | 2.301(3)  | 2.302(3)  | 2.324(3)  | 2.328(3)  | 2.328(3)  | 2.347(3)   | 2.364(3)  | 2.380(4)   | 2.463(4)   | 2.471(4)   |
|       | -0(2)×2 | 1.927(0)  | 1.927(0)  | 1.926(0)  | 1.927(0)  | 1.928(0)  | 1.928(0)   | 1.930(0)  | 1.930(1)   | 1.941(0)   | 1.940(0)   |
|       | -0(3)×2 | 1.961(0)  | 1.960(0)  | 1.959(0)  | 1.959(0)  | 1.958(0)  | 1.957(1)   | 1.954(0)  | 1.951(1)   | 1.941      | 1.940      |
|       | - V     | 2.209( 1) | 2.212( 1) | 2.203( 1) | 2.197(1)  | 2.196( 1) | 2.187(3)   | 2.179(1)  | 2.181(6)   | 2.127(1)   | 2.134(1)   |
| O(1)  | - V     | 2.015(4)  | 1.991(4)  | 1.992(4)  | 1.996(4)  | 1.985(4)  | 1.975(7)   | 1.984(4)  | 1.993(11)  | 1.942(11)  | 1.937(11)  |
| O(2)  | - V     | 2.030(3)  | 2.040(2)  | 2.043(2)  | 2.044(2)  | 2.044(2)  | 2.050(3)   | 2.049(3)  | 2.046(8)   | 2.058(3)   | 2.072(3)   |
| O(3)  | - V     | 0.014(4)  | 2.023(4)  | 2.026(4)  | 2.027(4)  | 2.030(4)  | 2.036(9)   | 2.036(3)  | 2.033( 10) | 2.058(3)   | 2.072(3)   |
| O(4)  | - V     | 1.798( 1) | 1.770(1)  | 1.762(1)  | 1.755( 1) | 1.742(1)  | 1.730( 1)  | 1.725( 1) | 1.723(1)   | 1.621(1)   | 1.604( 1)  |
| Cat   | - V     | 14.08(3)  | 13.78(3)  | 13.73(3)  | 13.68(3)  | 13.53(3)  | 13.33(5)   | 13.22(3)  | 12.96(7)   | 12.68(4)   | 12.06(4)   |
| Oxy   | - V     | 13.83(2)  | 13.60(2)  | 13.545(2) | 13.50(2)  | 13.39(2)  | 13.23(4)   | 13.14(2)  | 12.92(6)   | 12.68(3)   | 12.18(3)   |

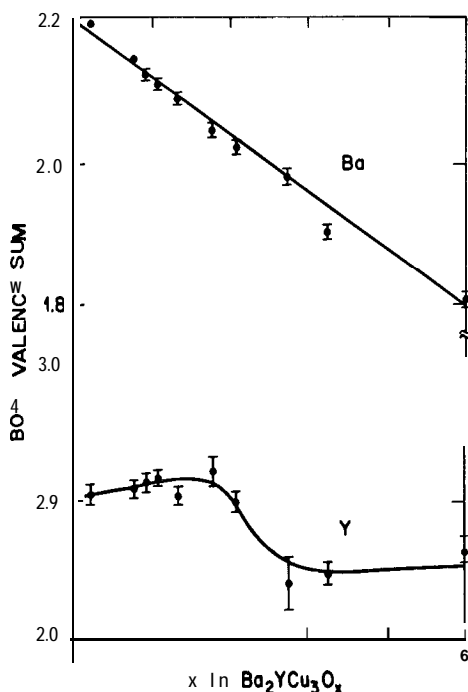


Fig. 14. Bond valence sums around Ba and Y as a function of oxygen stoichiometry.

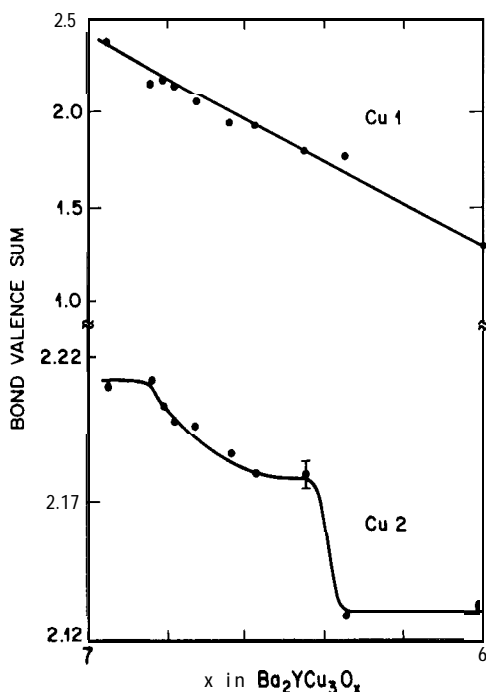


Fig. 15. Bond valence sums around the chain coppers (Cu(1)) and plane coppers (Cu(2)) as a function of oxygen stoichiometry.

Consider first the atoms Y and Ba which are expected to have ionic bonds to oxygen with fixed valences of +3 and +2. Fig. 14 shows that the Y bond valence sum is near 2.9, which represents a reasonable agreement with +3 given the hybridization of the oxygens. Overall, the value in the orthorhombic phase is slightly higher than that for the tetragonal or nearly tetragonal samples. That this is due to a change in the geometrical structural constraints is suggested by fig. 11, which shows that the Y-O(2) bondlength is nearly constant over the whole stoichiometry range, while the Y-O(3) bondlength rises to meet it at the orthorhombic to tetragonal transition. In contrast, fig. 11 shows that the Ba-O(2) and Ba-O(3) bondlengths track together through the orthorhombic phase, and that their average extrapolates linearly to their common value at  $x=6.0$ . This translates into a linear Ba bond valence sum, shown in fig. 14, where again the variation from 2.2 to 1.8 can be interpreted as a change in geometric stress (the coordination polyhedron is too small for Ba at  $x=7$  and too large at  $x=6$ ) imposed by the rest of the structure [25]. Models which take into account the internal geometrical stress yield the expected composition independent  $2+$  bond valence sum for Ba [25].

The bond valence sums around the planar and chain coppers are considerably more interesting. The values shown in fig. 15 are of course meaningful when compared to each other, and if corrected for internal geometric stresses, would shift by a small composition independent amount which would result in the plane and chain copper valences being  $2+$  and  $1+$  in  $Ba_2YCu_3O_6$  [25]. A dramatic difference in the oxygen stoichiometry dependence of the electronic charge associated with chain and plane coppers is observed. The charge associated with the chain coppers decreases in a linear manner with decreasing oxygen content over the whole stoichiometry range, independent of the symmetry of the phase and whether the material is superconducting or semiconducting. The change in charge is dominated by the removal of oxygen from the bonding environment of copper as the oxygen content varies from 7 to 6.

In contrast, the charge associated with the plane copper displays a remarkable nonlinear variation with oxygen stoichiometry. The total positive charge decreases by about  $0.08e$  per plane copper as  $x$  decreases from 7 to 6. For  $x > 6.8$  the charge is ap-

proximately constant. As oxygen is removed below 6.8 there is a gradual decrease in charge reaching a plateau near  $x=6.5$  before there is a precipitous drop of  $0.05e$  per plane copper between oxygen contents of  $x=6.45$  and 6.35. The charge associated with the plane coppers is then constant in the tetragonal phase for  $6.35 < x < 6.0$ .

Fig. 16 compares the bond valence sum of Cu (2) and the superconducting transition temperature for  $Ba_2YCu_3O_x$  for  $7 > x > 6$ . The correlation is obvious: the bond valence sum shows the same two plateau behaviours as does  $T_c$  versus  $x$ . Thus the change from a 90 K to a 60 K superconductor is due to decrease in positive charge associated with the plane Cu(2) layer of approximately  $0.03e/Cu$ , a reduction of the "hole" concentration. This is the first time this correlation could be so clearly made. The transition from 60 K superconductor to semiconductor involves an abrupt decrease in positive charge in the plane Cu (2) layer of approximately  $0.05e/Cu$ .

Finally, the data in fig. 15 give some information on another important issue: how the charge is distributed as oxygen is added to the antiferromagnetic semiconductor  $YBa_2Cu_3O_6$ . The positive charge as-

sociated with the addition of oxygen is accompanied entirely in the chain coppers. Apparently, no holes are doped into the  $CuO_2$  layer until the superconducting state appears at  $x=6.45$ . Therefore, any observed variation of  $T_N$  with composition in the tetragonal phase must be a secondary effect due for instance to increased electronic coupling between the plane coppers via the changing chain coppers.

## 9. Conclusion

We have presented the results of superconducting property measurements, electron diffraction studies of oxygen ordering, and powder neutron diffraction determinations of the average crystal structures for oxygen deficient  $Ba_2YCu_3O_x$  prepared at  $440^\circ C$  by Zr-gettered annealing. The variation of copper oxygen bondlengths with stoichiometry points to a continuous linear variation of the charge associated with the chain coppers and a nonlinear variation of charge associated with the plane coppers. The bond valence sum around the plane copper, a representation of the total charge associated with the  $CuO$  pyramidal planes, shows the same oxygen stoichiometry dependence as does the two-plateau superconducting transition temperature. We can conclude that the decrease of  $T_c$  from 90 K to 60 K is due to a transfer of (negative) charge of approximately  $0.03e/Cu$  into the planes near  $x=6.6$ , and that the superconductivity disappears when a further  $0.05e/Cu$  (negative) charge is transferred to the planes near  $x=6.45$ . Further, on the addition of oxygen to  $Ba_2YCu_3O_6$ , our results suggest that no holes appear on the  $Cu-O$  pyramidal planes until superconductivity abruptly appears near  $x=6.45$ . The concept of charge transfer controlling  $T_c$  in  $Ba_2YCu_3O_x$ , and the role of the  $Cu-O$  chains as a charge reservoir, appears now to be clearly established. In addition to the structural  $T_c$  correlations discussed here and in ref. [6], study of the crystal field splitting of the rare earth 4f electrons [26] is also sensitive to this charge transfer, and is in full agreement with our picture. The electron microscopy studies show that short range oxygen ordering with various repeat distances appears as oxygen is removed from  $Ba_2YCu_3O_7$  at the same stoichiometry where  $T_c$  begins to drop from 90 K. For these materials, a three-dimensionally ordered  $2a$  supercell, presumably corresponding to ordering of full and empty  $Cu-O$  chains, dominates in the SEC-

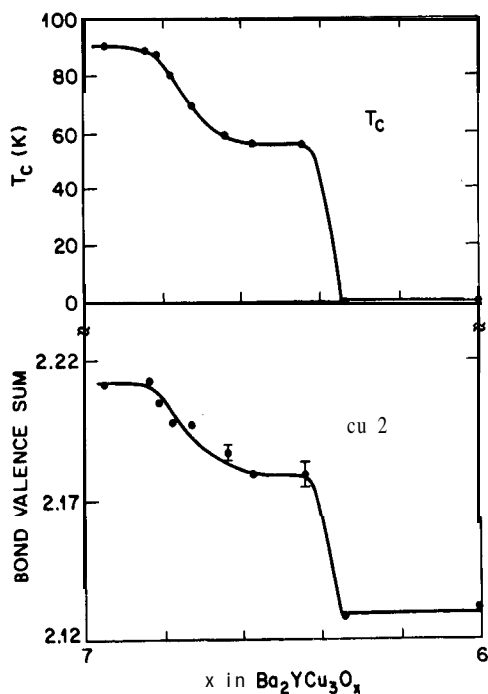


Fig. 16. Comparison of  $T_c$  and bond valence sum around the plane copper as a function of oxygen stoichiometry.

ond plateau region ( $\approx 55$  K in these samples) of  $T_c$  versus  $x$  near  $x = 6.6-6.45$ . In the stoichiometry region between 6.8 and 6.6, where the oxygen ordering periodicity is changing quickly, the superconducting transitions broaden, suggesting the presence of a distribution of  $T_{c's}$  between 90 K and 60 K. We propose that each different short range ordering scheme has its own characteristic  $T_c$  between 90 K and 60 K, and that their similarity in composition makes their isolation in pure form difficult. The fact that one of our samples in this composition region shows two distinct  $T_{c's}$  suggests that better isolation may be possible.

We believe that for all the results reported in the literature for oxygen deficient  $Ba_2YCu_3O_x$ , special care must be paid to the method of synthesis of the samples. In particular, due to the presence of many possible stable or metastable long range or short range oxygen configurations in the chains, the temperature of the synthesis is critical. For equally carefully done studies, there are a variety of "correct" physical properties or structural configurations at any particular oxygen stoichiometry. In this context, comparison of our results to the recently completed study by Jorgensen et al. [27] on samples quenched from 520°C will prove to be of considerable interest. It is clear that nature has provided us with an unexpectedly interesting compound in  $Ba_2YCu_3O_x$ , with many questions about the detailed behaviour with oxygen stoichiometry yet to be answered.

## References

- [1] R.J. Cava, B. Batlogg, C.H. Chen, E.A. Rietman, S.M. Zahurak and D. Werder, *Phys. Rev. B* 36 (1987) 5719; *ibid.*, *Nature* 329 (1987) 423.
- [2] D.C. Johnston, A.J. Jacobson, J.M. Newsam, J.T. Lewandowski, D.P. Goshorn, D. Xie and W.B. Yelon, in: *Chemistry of High-Temperature Superconductors*, eds. D.L. Nelson, M.S. Whittingham and T.F. George, ACS Symposium Series 351 (Amer. Chem. Soc., Washington, DC, 1987) p. 136.
- [3] J.M. Tarascon, P. Barboux, B.G. Bagley, L.H. Greene, W.R. McKinnon and G.W. Hull, in: *Chemistry of High Temperature Superconductors*, eds. D.L. Nelson, M.S. Whittingham and T.F. George, ACS Symposium Series 35 1, (Amer. Chem. Soc., Washington, DC, 1987) p. 198.
- [4] J.M. Tarascon, L.H. Greene, B.G. Bagley, W.R. McKinnon, P. Barboux and G.W. Hull, in: *Novel Superconductivity*, eds. S.A. Wolf and V.Z. Kresin (Plenum Press, New York and London, 1987) p. 705.
- [5] R. Beyers, G. Lim, E.M. Engler, V.Y. Lee, M.L. Ramirez, R.J. Savoy, R.D. Jacowitz, T.M. Shaw, S. La Placa, R. Boehme, C.C. Tsuei, S.I. Park, M.W. Shafer and W.J. Gallagher, *Appl Phys. Lett.* 5 1 (1987) 6 14.
- [6] R.J. Cava et al., *Physica C* 153-155 (1988) 560; R.J. Cava, B. Batlogg, K.M. Rabe, E.A. Rietman, P.K. Gallagher and L.W. Rupp Jr., *Physica C* 156 (1988) 523.
- [7] Y. Ueda and K. Kosuge, *Physica C* 156 (1988) 281.
- [8] J.D. Jorgensen, B.W. Veal, W.K. Kwok, G.W. Crabtree, A. Umezawa, L.J. Nowicki and A.P. Paulikas, *Phys. Rev. B* 36 (1987) 5731.
- [9] W.K. Kwok, G.W. Crabtree, A. Umezawa, B.W. Veal, J.D. Jorgensen, S.K. Malik, L.J. Nowicki, A.P. Paulikas and L. Nunez, *Phys. Rev. B* 37 (1988).
- [10] D.J. Werder, C.H. Chen, R.J. Cava and B. Batlogg, *Phys. Rev. B* 37 (1988) 2317; *ibid.*, *Phys. Rev. B* 38 (1988) 5130.
- [11] R.M. Fleming, L.F. Schneemeyer, P.K. Gallagher, B. Batlogg, L.W. Rupp and J.V. Waszczak, *Phys. Rev. B* 37 (1988) 7920.
- [12] M.A. Alario-Franco, C. Chailout, J.J. Capponi, J. Chenavas and M. Marezio, *Physica C* 156 (1988) 455.
- [13] C.H. Chen, D.J. Werder, L.F. Schneemeyer, P.K. Gallagher and J.V. Waszczak, *Phys. Rev. B* 38 (1988) 2888.
- [14] R. Beyers, B.T. Ahn, G. Gorman, V.Y. Lee, S.S.P. Parkin, M.L. Ramirez, K.P. Roche, J.E. Vazquez, T.M. Gur and R.A. Huggins, *Nature* 340 (1989) 619.
- [15] H.W. Zandbergen, G. Van Tendeloo, T. Okabe and S. Amelinckx, *Phys. Status Solidi A* 103 (1987) 45.
- [16] M.A. Alario-Franco, J.J. Capponi, C. Chailout, J. Chenavas and M. Marezio, in: *High Temperature Superconductor*, eds. M.B. Brodsky, R.C. Dynes, K. Kitazawa and H.L. Tuller, *Mat. Res. Soc. Symp. Proc.* 99 (1987) 4 1.
- [17] A.W. Hewat, *Mat. Sci. Forum* 9 (1986) 69.
- [18] M. Francois, A. Junod, K. Yvon, A.W. Hewat, J.J. Capponi, P. Strobel, M. Marezio and P. Fischer, *Solid State Commun.* 66 (1988) 1117.
- [19] A.W. Hewat, UKAEA Harwell report R7350 (1973).
- [20] J.J. Capponi, C. Chailout, A.W. Hewat, P. Lejay, M. Marezio, N. Nguyen, B. Raveau, J.L. Soubeyrou, J.L. Tholence and R. Toumier, *Europhys. Lett.* 3 (1987) 1301.
- [21] J.T. Willie, A. Berera and D. de Fontaine, *Phys. Rev. Lett.* 60 (1988) 1065.
- [22] A.G. Khachatryan and J.W. Morris Jr., *Phys. Rev. Lett.* 61 (1988) 215.
- [23] V.E. Zubkus, S. Lapinskas and E.E. Tomeau, *Phys. Status Solidi*, to be published.
- [24] I.D. Brown and D. Altermatt, *Acta Crystallogr.* B4 1 (1985) 244.
- [25] I.D. Brown, *J. Solid State Chem.* 82 (1989) 122.
- [26] P. Allenspach, A. Furrer and B. Rupp, in: "Proc. Int. Seminar on High Temperature Superconductivity, Dubna USSR, 28 June- 1 July 1989 (World Scientific Publ. Comp., Singapore, 1989), in press.
- [27] J.D. Jorgensen, B.W. Veal, A.P. Paulikas, L.J. Nowicki and G.W. Crabtree, *Phys. Rev. B*, submitted.